ORIGINAL PAPER

Andres Rüggeberg · Christian Dullo · Boris Dorschel ·
Dierk Hebbeln

Environmental changes and growth history of a cold-water carbonate mound (Propeller Mound, Porcupine Seabight)

Abstract On- and off-mound sediment cores from Propeller Mound (Hovland Mound province, Porcupine Seabight) were analysed to understand better the evolution of a carbonate mound. The evaluation of benthic foraminiferal assemblages from the off-mound position helps to determine the changes of the environmental controls on Propeller Mound in glacial and interglacial times. Two different assemblages describe the Holocene and Marine Isotope Stage (MIS) 2 and late MIS 3 (∼31 kyr BP). The different assemblages are related to changes in oceanographic conditions, surface productivity and the waxing and waning of the British Irish Ice Sheet (BIIS) during the last glacial stages. The interglacial assemblage is related to a higher supply of organic material and stronger current intensities in water depth of recent coral growth. During the last glaciation the benthic faunas showed high abundances of cassidulinid species, implying cold bottom waters and a reduced availability of organic matter. High sedimentation rates and the domination of *Elphidium excavatum* point to shelf erosion related to sea-level lowering (∼50 m) and the progradation of the BIIS onto the shelf. A different assemblage described for the on-mound core is dominated by *Discanomalina coronata*, *Gavelinopsis translucens*, *Planulina ariminensis*, *Cibicides lobatulus* and to a lower degree by *Hyrrokkin sarcophaga*. These species are only found or show significantly higher relative abundances in on-mound samples and their maximum contribution in the lower part of the record indicates a higher coral growth density on Propeller Mound in an earlier period. They are less abundant during the Holocene, however. This dataset portrays the boundary conditions of the habitable range for the cold-water coral *Lophelia pertusa*, which dominates the deep-water reefal ecosystem on the upper flanks of Propeller Mound. The growth of this ecosystem occurs during interglacial and interstadial periods, whereas a retreat of corals is documented in the absence of glacial sediments on-mound. Glacial conditions with cold intermediate waters, a weak current regime and high sedimentation rates provide an unfavourable environmental setting for *Lophelia* corals to grow. A Late Pleistocene decrease is observed in the mound growth for Propeller Mound, which might face its complete burial in the future, as it already happened to the buried mounds of the Magellan Mound province further north.

Keywords Carbonate mounds · Cold-water corals · Mound development · Paleo-environment · Porcupine Seabight · NE Atlantic

A. Rüggeberg (✉) · C. Dullo
IFM-GEOMAR, Leibniz-Institute of Marine Sciences,
Wischhofstraße 1–3, 24148 Kiel, Germany
E-mail: arueggeberg@ifm-geomar.de

B. Dorschel · D. Hebbeln
Department of Geology, University of Bremen, Postbox 330440,
28334 Bremen, Germany

Introduction

Carbonate mounds along the European continental margin have been the subjects of intense research during the past decade. The Propeller Mound in the Porcupine Seabight (PSB) has been intensively sampled and studied during several cruises within the period of 2000 and 2002 (Freiwald et al. 2000; De Mol 2002; De Mol et al. 2002; Freiwald and Shipboard Party 2002). This mound is part of a cluster of high elevated mounds (upto 150 m) in the Hovland Mound province (Fig. 1). North to that area, seismic surveys detected a cluster of buried mounds—the Magellan Mound province—with the sediment cover on the mounds pointing to strong sediment transport from the surrounding shallower shelf areas (De Mol 2002; Huvenne et al. 2002). At the eastern slope of the PSB to the SE of the Hovland and Magellan Mounds the Belgica Mound province is located, including mounds upto 190 m high (Henriet et al. 1998; De Mol et al. 2002).

Propeller Mound shows strongly current-induced features, like the N–S elongation, the steep flanks (upto 45°) and the moats around the foot of the mound (De Mol 2002; Freiwald 2002). Underwater investigations using the ROV CHEROKEE of Bremen University (Freiwald and Shipboard Party 2002) clearly show the sediment distribution on the mound. It is mainly covered by dead coral debris in a sandy silty matrix. Recent coral growth is restricted to the upper flanks of the mound (690–710 m water depth), where a dense living coral ecosystem occurs. However, close to the studied on-mound core GeoB 6730-1 (Fig. 1) only patches of living corals have been observed. The coral thickets on Propeller Mound are mainly built up by cold-water corals *Lophelia pertusa*, *Madrepora oculata* and to a minor degree by *Desmophyllum cristagalli* (Freiwald 2002).

The recent mound growth is strongly controlled by the present oceanographic setting, which is described in detail by White (this volume). A generally northward transport of water masses west of Ireland is documented at the surface and in mid-water depths (< 1,000 m). At depth of recent coral growth in the Hovland Mound province (600–800 m), a water mass boundary occurs between the Eastern North Atlantic Water (ENAW, Pollard et al. 1996) and the Mediterranean Outflow Water (MOW). A branch of ENAW and MOW enters the PSB (Mohn 2000) and flows topographically steered cyclonically around the slope within the PSB (Ellet et al.
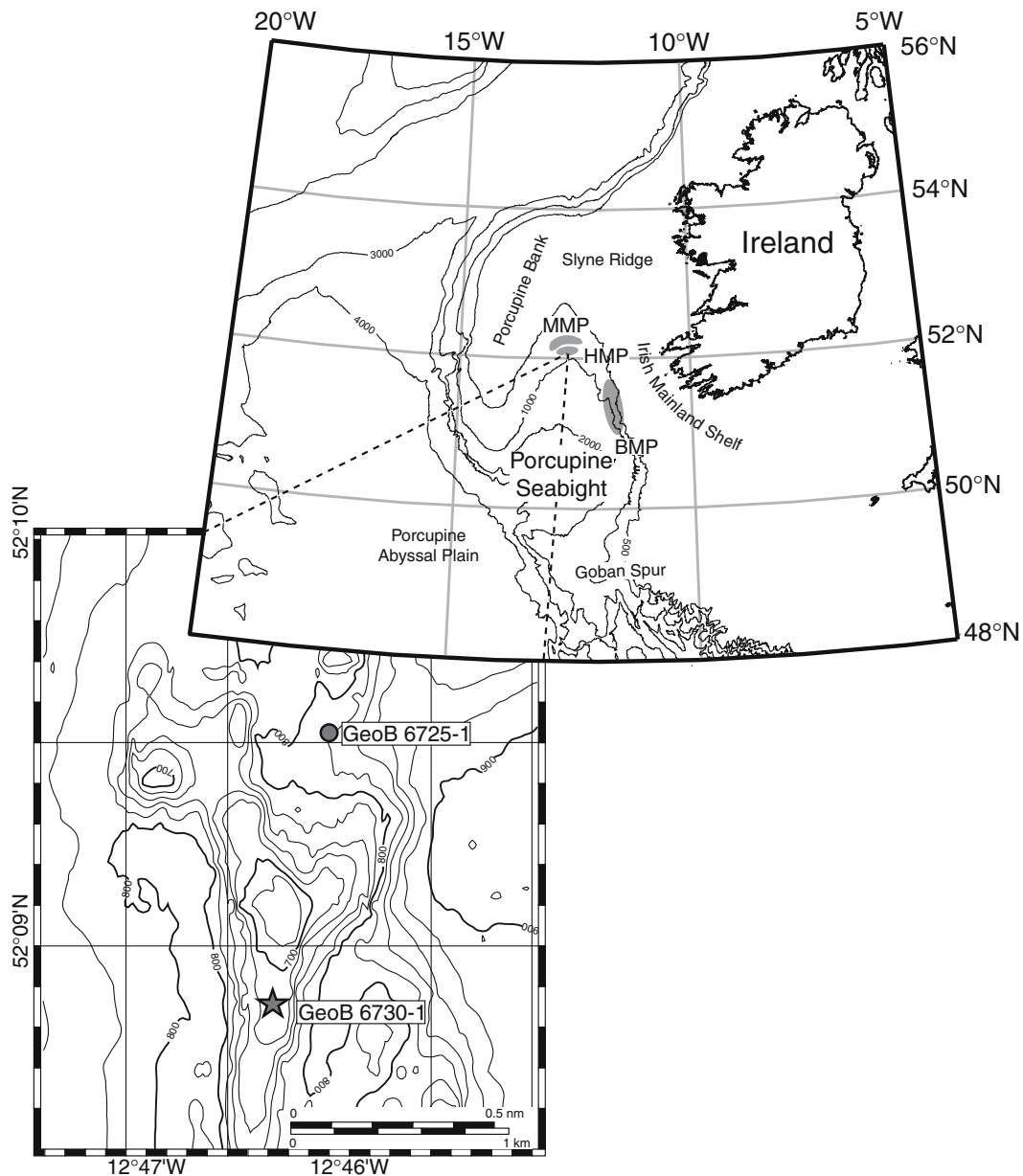
Fig. 1 Location map of Propeller Mound with sediment core sites analysed within this study. *Star* = on-mound core GeoB 6730-1, *circle* = off-mound core GeoB 6725-1

1986). At the northern end of the PSB, where the Hovland and Magellan Mounds are situated, the currents are relatively weaker (1–5 cm/s) and turn into a southward flow (White 2001). It has been suggested that MOW does not penetrate to any large degree further poleward in the Rockall Trough north of Porcupine Bank (New et al. 2001; McCartney and Mauritzen 2001). During RV POSEIDON cruise 265 in 2000, several CTD profiles above the Propeller Mound show an increase in salinity below 600 m (De Mol 2002). Due to a strong gradient in density at this water–mass interface, organic material from the sea surface persists at this level for a longer time. In addition, it is also transported laterally within the PSB by currents generally flowing at around 5 cm/s with maximum velocities upto 40 cm/s (White 2001 this volume). The corals benefit from this enrichment of food particles at the density-driven interface between the two water masses. It is obvious that water mass variations during glacial–interglacial cycles, where major differences of the oceanographic setting existed, had a great impact on coral growth and distribution.

Glacial oceanographic setting

The glacial oceanographical setting is not well studied in the PSB. The North Atlantic Polar Front was situated south of the PSB during most of last glacial stages (Jones and Keen 1993). Surface water movement was reversed during glacials, flowing southward as a coastal current west off Ireland (Fig. 2; Sarnthein et al. 1995), leading to summer sea surface temperatures (SSTs) of 5°C for the last glacial maximum (LGM) (< 6°C for most of MIS 3) and winter SSTs of 0–1°C (2–8°C) (Sarnthein et al. 1995; Bowen et al. 2002). Glacial North Atlantic Intermediate Water (GNAIW) occurred in water depths down to 1,700–2,000 m (Manighetti and McCave 1995) and flowed from the north via the Wyville–Thomson Ridge and through the Rockall Trough to the south. According to Duplessy et al. (1988) and Oppo and Lehman (1993) the term GNAIW is used for mid-depth waters of uncertain origin. Its production occurred in the Norwegian Sea at least during MIS 2 via a mechanism strongly influenced by sea ice formation (Veum et al. 1992), but the composition of GNAIW may have changed during the glacial time with differing sources. An influence of the very cold GNAIW on the PSB is assumed. Schönfeld and Zahn (2000) describe a main glacial MOW flow upto 800 m deeper than today, due to an increased density induced by a much higher salinity. In addition, the glacial flow pattern indicates no advection of MOW along the European continental margin beyond Iberia. It is therefore less likely that any strong density gradient

Fig. 2 General map of Ireland during glacial intervals. Indicated are ice limits (*dark blue*) and general ice-flow (*black arrows*) for MIS 2 (after Eyles and McCabe 1989; Jones and Keen 1993), maximum land-ice extension (*light blue*) for MIS 4 (after Bowen et al. 2002), surface circulation (*grey arrows*) and melt water intrusion (MW) resulting in a week anticyclonic circulation around Rockall Bank for MIS 2 (after Sarnthein et al. 1995). N–S trending iceberg ploughmarks are reported on Slyne Ridge (after Games 2001). Glacial bathymetry corresponds to present-day water depth minus 120 m. *Red dot* marks the position of Propeller Mound
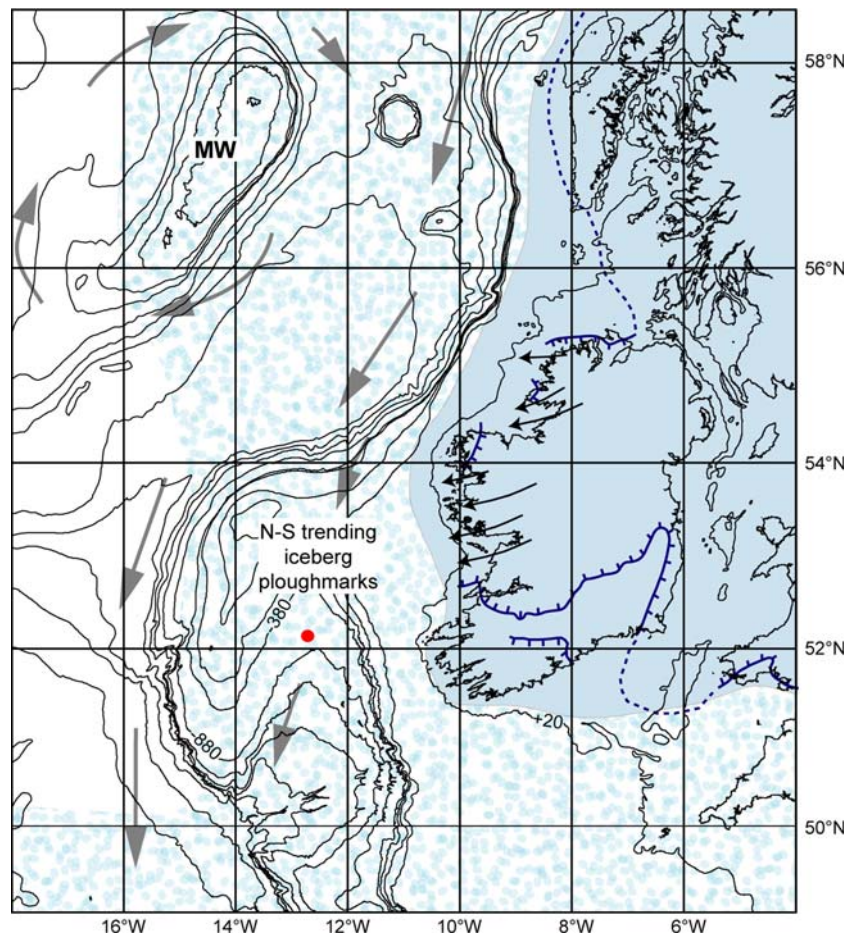
like today existed in the glacial intermediate water column and MOW existed in the PSB.

A maximum land–ice extension of the BIIS probably reaching offshore West Ireland to the present 200 m isobath is reported by Bowen et al. (2002) for MIS 4 (Fig. 2). During MIS 3 Ireland was covered with treeless, tundra-like vegetation (Jones and Keen 1993). An advance of land-ice occurred around 30 ka BP, covering most of Ireland (Knutz et al. 2001) synchronous with a sea-level lowering of around 50 m (Lambeck et al. 2002). The southward flowing surface waters, land-ice extension and calving of icebergs from Irish mainland as documented by ice berg plough marks on Slyne Ridge (Games 2001), as well as the sea-level lowering suggest an enormous increase in terrigenous sediment supply to the PSB comparable to the Celtic margin further south (Auffret et al. 2002).

The objectives of this study are to reconstruct the environmental setting of Propeller Mound for the past glacial–interglacial cycle, to resolve disturbances of the general sedimentation, related to episodes of sea-level lowering and advances of land–ice masses on Ireland inducing calving of icebergs, as well as paleoceanographic changes between glacial–interglacial times. Evidence is inferred by stable oxygen isotope data, AMS ^{14}C and U/Th datings, total and organic carbon measurements, as well as the evaluation of benthic foraminiferal assemblages from an off-mound location (core GeoB 6725-1) and an on-mound (core GeoB 6730-1) location.

Materials and methods

Two sediment cores from the Propeller Mound region, GeoB 6725-1 (off-mound position 52°09.52′N, 12°46.01′W; water depth 820 m) and GeoB 6730-1

(on-mound position 52°08.86′N, 12°46.28′W; water depth 704 m; see Fig. 1) were chosen for the present study. Both cores were sampled every 5 cm using 10 ml syringes. Each sample was weighed, carefully washed over 63 µm sieves, dried at 50°C and weighed again. Thereafter all samples were dry sieved into fractions 63–125, 125–250, 250–500, 500–1,000 and >1,000 µm. Fractions >125 µm were used for faunal analysis. A taxonomic list of benthic foraminiferal species discussed in this study is given in Appendix 1. SEM images of most of these species are illustrated in Plate 1 of Appendix 2. Species diversity is expressed in numbers of species corrected to an equal size of 100 specimens (Lutze 1980).

For the analysis of total organic carbon (TOC) and total carbon (TC) the samples were measured using a Carlo Erba NA-1500-CNS analyser at GEOMAR, Kiel. Organic carbon is determined after removing carbonate carbon by acidification with 0.01[Ntn] hydrochloric acid. Inorganic carbon was derived from the difference between total and organic carbon. Weight-percent carbonate was calculated according to their atomic weight ratios as $CaCO_3$ (%) = $8.33 \times (TC - TOC)$.

Stable oxygen isotopes ($\delta^{18}O$) were measured on three to five specimens of either the benthic foraminifera *Cibicidoides kullenbergi* or *Cibicidoides wuellerstorfi* (fraction 250–500 µm) for both investigated cores. Additionally, 15 specimens per sample of planktonic foraminifera *Globigerina bulloides* (fraction 250–315 µm) have been analysed for their $\delta^{18}O$ composition for the top 120 cm of off-mound core GeoB 6725-1, as limited numbers of this species were present in intervals below 120 cm. The isotopic composition of the samples was carried out with a Finnigan MAT 251 mass spectrometer at the Isotope Lab at Bremen University. A working standard (Burgbrohl CO_2 gas) was applied, which has been calibrated against PDB by using the NBS 18, 19

Fig. 3 Stratigraphy of off-mound core GeoB 6725-1 from benthic and planktonic oxygen isotope data, *star* = AMS ^{14}C dates, *circle* = inter-core correlation (Dorschel et al. this volume). Also indicated are the carbonate and organic carbon contents, concentration (# of ind/g) and diversity (# species) of benthic foraminifera, as well as the core lithology
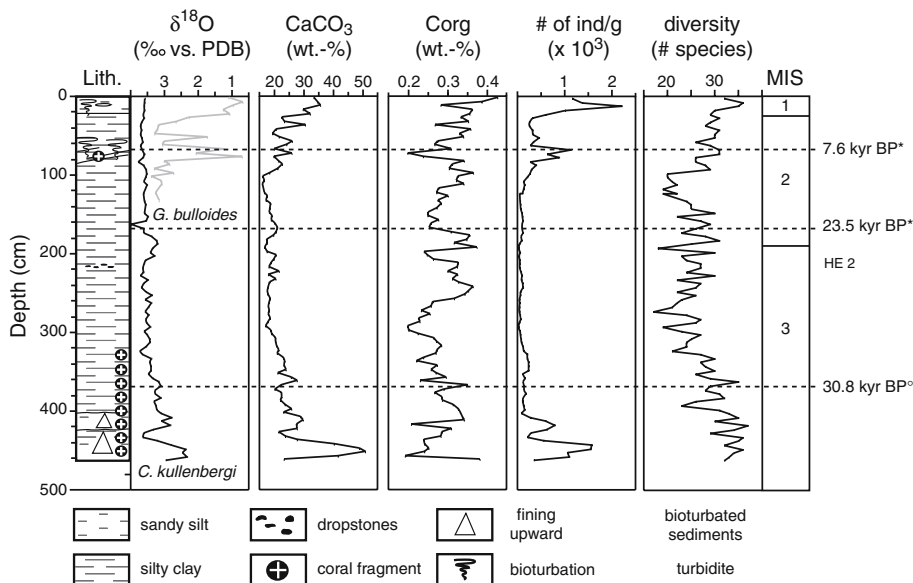
and 20 standards. Consequently, all δ^{18}O data given here are relative to the PDB standard. Analytical standard deviation is about $\pm 0.07\permil$.

Age estimations in both cores are based on AMS ^{14}C datings using monospecies samples of planktic foraminifera species *Neogloboquadrina pachyderma* (either dextral or sinistral) from the fraction 125–250 μm. Approximately 10 mg of foraminiferal carbonate were analysed at the Leibniz Laboratory for Age Determinations and Isotope Research at the University of Kiel (Nadeau et al. 1997). After the correction for δ^{13}C, the ^{14}C ages were calibrated to the calendar year scale by the Calib 4.3 program (Stuiver and Reimer 1993) using the marine dataset of Stuiver et al. (1998) and a reservoir age of 400 years. Ages greater 21 kyr BP were corrected using the method of Voelker et al. (1998) (see Table 2 in Dorschel et al. this volume).

In several depth intervals of core GeoB 6730-1 some coral fragments of *L. pertusa* were used to determine additional absolute ages using the U/Th ratio of the aragonite skeleton (see Table 3 in Dorschel et al. this volume). All samples were first ultrasonically cleaned and scrubbed with dental tools to remove exterior contaminants (iron–manganese crusts and coatings) from the fossil coral fragments as described in Cheng et al. (2000). When the coral looked clean under the binocular, each sample was bathed in 50/50 mixture of 30% peroxide and 1 M NaOH for 15 min with ultrasonification to remove organic stains left on the coral. Before the measurements using a Finnigan MAT 262 RPQ2+ thermal ionisation mass spectrometer at IFM-GEO-

MAR Kiel, all samples were checked for the cleanness of the aragonite. Therefore a little part of the samples was cut off before and after the chemical and physical cleaning and was analysed using X-ray diffraction, to evaluate the mineralogical composition primarily of the aragonite skeleton after the whole procedure (100% aragonite in all samples).

Results

Off-mound core GeoB 6725-1

Stratigraphy

Oxygen isotope data, carbon measurements, absolute abundance, as well as numbers of species of benthic foraminifera are illustrated in Fig. 3. The base of the core is disturbed by turbidites indicated by two sequences of upward fining sediments. Above this sequence the benthic δ^{18}O record shows low variability with values around $3.5\permil$ PDB. Planktonic δ^{18}O measurements within the top 120 cm present a higher variability with values ranging between 0.7 and $3.3\permil$ PDB. In general, lower δ^{18}O values of *G. bulloides* are synchronous with higher carbonate content (35%) of the foraminifera bearing sandy silt, whereas persistently low values of carbonate (20%) were found in fine-grained, terrigenous sediments below ~50 cm core depth. The mean carbonate content of the off-mound core is 22.5%. The absolute abundance and normalised diversity of benthic forami-
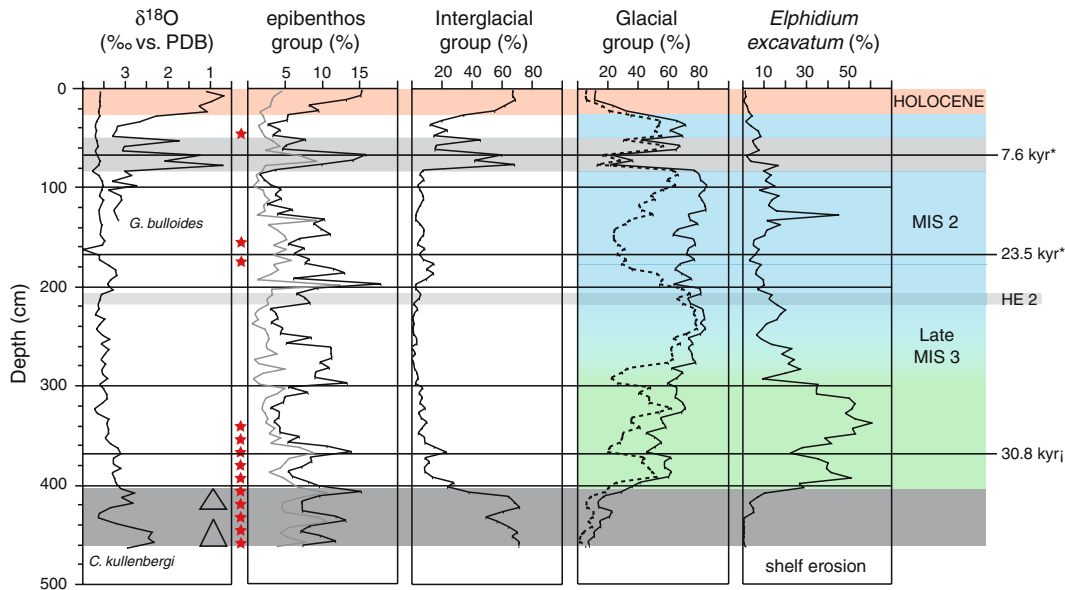
Fig. 4 Relative abundance of the interglacial group (*U. mediterranea, T. angulosa, M. barleeanum, H. balthica, B. robusta, B. marginata, C. laevigata, U. peregrina*), the glacial group in *black* [*C. teretis*(stippled), *G. subglobosa, C. reniforme, C. kullenbergi, C. obtusa, S. woodi*] and the dominance of *E. excavatum* for late MIS 3 in off-mound core GeoB 6725-1. Epibenthic (*black*) and attached epibenthic species (*grey*) are according to Murray (1991) and Schönfeld (1997, 2002a). *Red stars* mark intervals with occurrence of coral fragments and other shell fragments, *triangles* show upward fining sediment, *star* = AMS ^{14}C dates, *circle* = inter-core correlation (Dorschel et al. this volume). Note: Relative abundance of interglacial group, glacial group and *C. teretis* were calculated without *E. excavatum* to the total assemblage
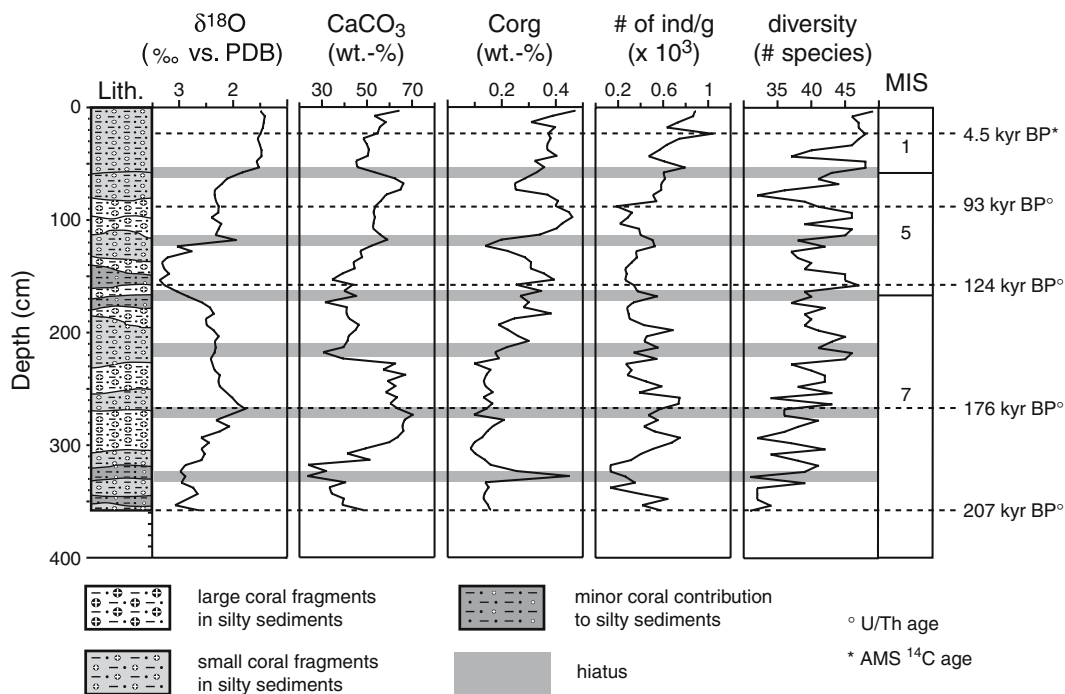
Fig. 5 Stratigraphy for on-mound core GeoB 6730-1 from benthic oxygen isotope data, AMS ^{14}C and U/Th dates. Also indicated are the records of carbonate and organic carbon contents, concentra-tion (# of ind/g) and diversity (# species) of benthic foraminifera, as well as the core lithology

nifera follow this trend, showing highest values at the core top (> 2,000 ind/g and > 30 species per sample) and lowest values in the fine-grained material (100–200 ind/g, 18–30 species per sample). Organic carbon contents (0.2–0.4%) are low throughout the core, again with the highest values recorded at the core top.

These data suggest a distribution into the youngest three marine isotope stages. Inter-core correlation of different off-mound cores (GeoB 6718-2, 6719-1) by Dorschel et al. (this volume) point out, that (1) a stratigraphic tie point, indicated by a characteristic double peak in the carbonate record, is probably related to Heinrich event H2 and its European precursor event, both dated to 23.7–25.6 cal kyr BP (Bond and Lotti 1995; Grousset et al. 2000; Bowen et al. 2002), and (2) that the turbidite sequence below 404 cm seems to be slightly older than 31 cal kyr BP. The sedimentation rate decreases from > 30 cm/kyr for the late MIS 3 to 10 cm/kyr for MIS 2, comparable to other near-shelf sites (e.g., Rasmussen et al. 2002b; Auffret et al. 2002; De Mol et al. 2002). The transition between MIS 2 and 3 (24 cal kyr BP) is set to 178 cm as documented in an AMS ^{14}C-date at 168 cm and a slight decrease in the benthic δ^{18}O values. The strong decline in δ^{18}O may indicate the Termination I. However, an additional AMS ^{14}C date at 68 cm represents an age of 7.65 cal kyr BP, pointing out an interval of heavily bioturbated sediments. The topmost 23 cm are consid-ered as Holocene because of lower δ^{18}O values of *G. bulloides*. This results in a sedimentation rate of 2–3 cm/kyr assuming the core top reflects the present-day sur-face sediment.

Benthic foraminiferal assemblages

The faunal diversity of benthic foraminifera in off-mound core GeoB 6725-1 is expressed in species number referred to an equal sample size of 100 counted speci-mens (Fig. 3). The values range from 20 species within MIS 2 to > 30 species during the Holocene.

Elphidium excavatum is highly abundant in off-mound core GeoB 6725-1, especially in the lower core part, where it exceeds 50% of total abundance (Fig. 4). This species is reported to live in shallow shelf areas generally above 200 m (Seidenkrantz et al. 2000), but is also found in greater depths to which it is often trans-ported passively. It belongs to the epiphytic taxa (Seidenkrantz et al. 2000), whereas Murray (1991) de-scribes non-keeled species of the genus *Elphidiidae* as infaunal, thriving free in mud and sand on the inner shelf. This species is most important in transitional cooling events (e.g., the Faeroe-Shetland Ridge, Ras-mussen et al. 1996) and is extremely tolerant and adaptable of large variations in temperature, salinity and food supply (Linke and Lutze 1993). It is widely dis-tributed in shallow polar seas (Hald et al. 1994) and known as an opportunistic species (Conradsen 1993; Steinsund and Hald 1994 for *E. excavatum* f. *clavatum*). Maximum concentrations of *Elphidiidae* species are ob-served in the proximity of river estuaries in the Barents and Kara Sea and in areas with heaviest ice cover (Steinsund and Hald 1994) and are associated with near glacial environments (Nagy 1965; Hald et al. 1994). The abundance of *E. excavatum* is considered as an indica-tion of erosional processes from shallow shelf areas and

therefore not a part of the fossil community (Struck 1992). Its abundance is not included into the calculation of the relative abundance of the following two assemblages.

The autochtonous benthic foraminiferal fauna of off-mound core GeoB 6725-1 shows two different assemblages depicting the Glacial and the Holocene. The Glacial group is dominated by *Cassidulina teretis*, *Globocassidulina subglobosa*, *Cassidulina reniforme*, *C. kullenbergi* and subdominant species *Cassidulina obtusa* and *Sigmoilopsis woodi*. This assemblage increases continuously from ~40% during late MIS 3 (mainly described by *C. teretis*) to values >80% during MIS 2 (Fig. 4). *C. teretis* is the most abundant species in this assemblage, varying between ~30% during the onset of MIS 2 and >70% within the peak glaciation (Fig. 4). This species is reported as shallow infaunal (Murray 1991), but also as epifaunal on sponge needles (Altenbach 1992), and feeds on organic debris at the surface or in the uppermost layer of the sediment (Korsun and Polyak 1989). Mackensen and Hald (1988) describe *C. teretis* as a continental slope species, thriving in cold bottom waters ($-1°C$) and preferring fine-grained, organic rich, terrigenous mud. The onset of MIS 2 is characterised by increasing abundance of *G. subglobosa*, *C. reniforme*, *C. kullenbergi*, *C. obtusa* and *S. woodi*, but their values decrease rapidly while *C. teretis* gets more abundant (Fig. 4). Those species may be interpreted as an indicator for cold and nutrient-poor bottom water conditions (Rasmussen et al. 2002b) and show an

infaunal habitat. *G. subglobosa* is reported in higher oxygen levels of the sediment pore water compared to the cassidulinid species (Kaiho 1994), but also tolerates high environmental stress, especially variations in the oxygen content (Seidenkrantz et al. 2000).

The Holocene interval is dominated by *Uvigerina mediterranea* and *Trifarina angulosa*. Subdominant species are *Melonis barleeanum*, *Hyalinea balthica*, *Bulimina marginata*, *Uvigerina peregrina* and *Cassidulina laevigata* (Fig. 4). This assemblage (interglacial group) has maximum relative abundances during the last 10 kyr BP and in deposits older than 30 kyr BP, but rarely exceeds 20% during MIS 2 or 3. In the bioturbated interval the interglacial group presents a comparable behaviour as the δ^{18}O record of *G. bulloides*, determining the existence of this heavily bioturbated section. Those species are reported as infaunal species (except *H. balthica*) living in muddy to fine sandy sediments (Murray 1991), whereas *T. angulosa* is associated with coarser sediments under the influence of stronger bottom currents (Mackensen et al. 1993, 1995; Rasmussen et al. 2002a).

On-mound core GeoB 6730-1

Stratigraphy

Figure 5 presents oxygen isotope data of *C. kullenbergi*, carbon measurements and absolute abundance, as well as numbers of species of benthic foraminifera from on-
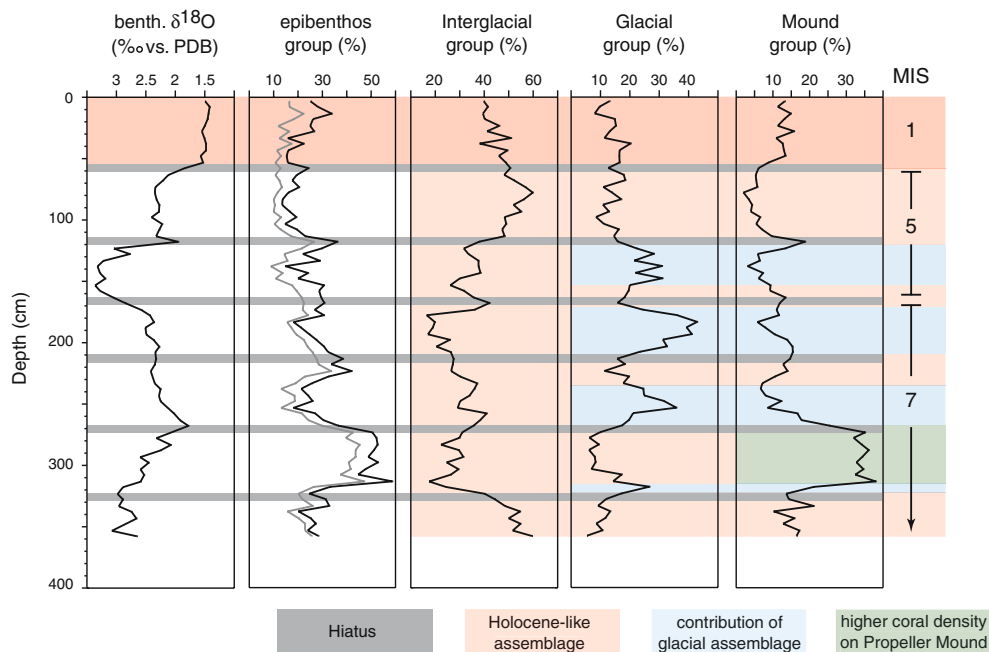
Fig. 6 Relative abundance of the off-mound-identified interglacial group and glacial group transferred to on-mound core GeoB 6730-1, as well as the Mound group and epibenthos group. Higher abundance of each assemblage describes the different sections illustrated to the right. Epibenthic (*black*) and attached epibenthic species (*grey*) are according to Murray (1991) and Schönfeld (1997, 2002a). Dominant and subdominant species of the Mound group are *D. coronata*, *G. translucens*, *C. lobatulus*, *H. sarcophaga*, *P. ariminensis*, *C. refulgens*, *T. bradyi*

mound core GeoB 6730-1. The δ^{18}O record is highly variable compared to the off-mound core, showing values between 1.4 and 3.4‰ PDB. In general, the carbonate content and absolute abundance of benthic foraminifera follows the δ^{18}O record with higher values during sections with low δ^{18}O values and vice versa. The carbonate content is more than twice as high as in the off-mound core (24–70%, mean = 50%), whereas organic carbon is generally low in abundance with values ranging between 0.1 and 0.4%. High numbers of species of benthic foraminifera (>45) occur at the core top and decrease towards the core base, but are generally highly diverse (mean = 40 species) than in the off-mound core GeoB 6725-1 (mean = 27 species).

The low benthic δ^{18}O values within the top 60 cm of the on-mound core GeoB 6730-1 as well as an AMS ^{14}C date of 4.5 cal kyr BP at 23 cm correspond to the Holocene interval (Fig. 5). Below the Holocene cover, the stable isotope record and several U/Th dates on coral fragments of *L. pertusa* indicate that the on-mound core represents a rather non-continuous sedimentation with almost no fully interglacial sediments (expected δ^{18}O values of around 1.5‰ PDB), nor glacial sediments (expected δ^{18}O values of >3.5‰ PDB) being preserved. Most likely, erosional processes on elevated mound areas with non-deposition or even removal of nearly all glacial and interglacial sediments during phases of enhanced current intensity may have caused these hiatuses. Therefore, core GeoB 6730-1 can only be divided into a Holocene cover and Pleistocene sediments below, probably into late Stage 7.

Fig. 7 The model Mound Factory describes mound growth during interglacial–glacial cycles of the Pleistocene, revealed from reconstructions of the environmental setting locked in sediments on- and off-mound of Propeller Mound. The Mound Factory follows the cycle of interglacial/interstadial mound growth, glacial retreat of corals and stagnation of mound growth, and the re-settlement of corals during terminations with the introduction of the recent oceanographic regime. Within *boxes*, key factors of the environmental control are indicated (+high/strong; −low/weak). *Below*, the present-day situation of Propeller Mound is indicated with the proposed future development
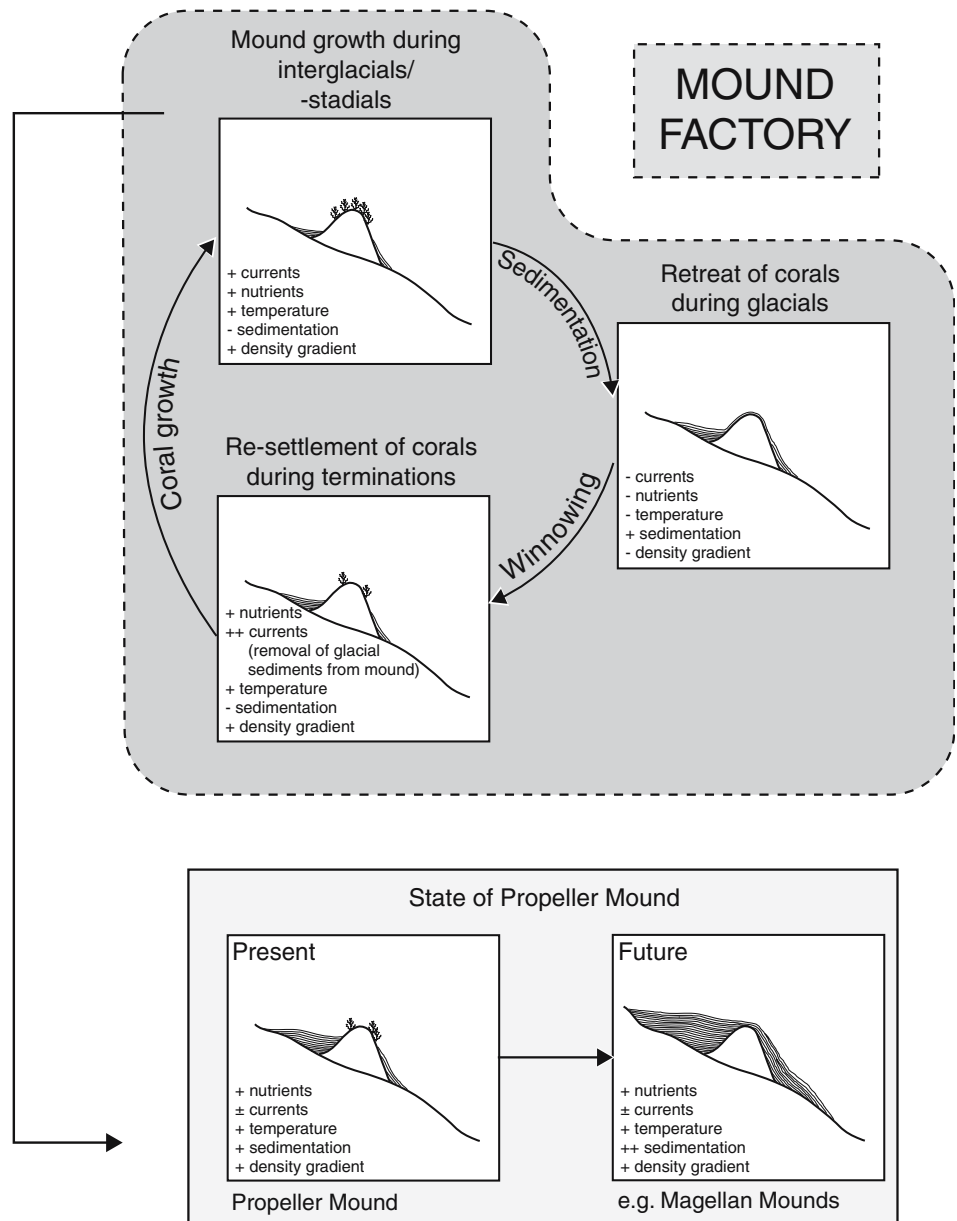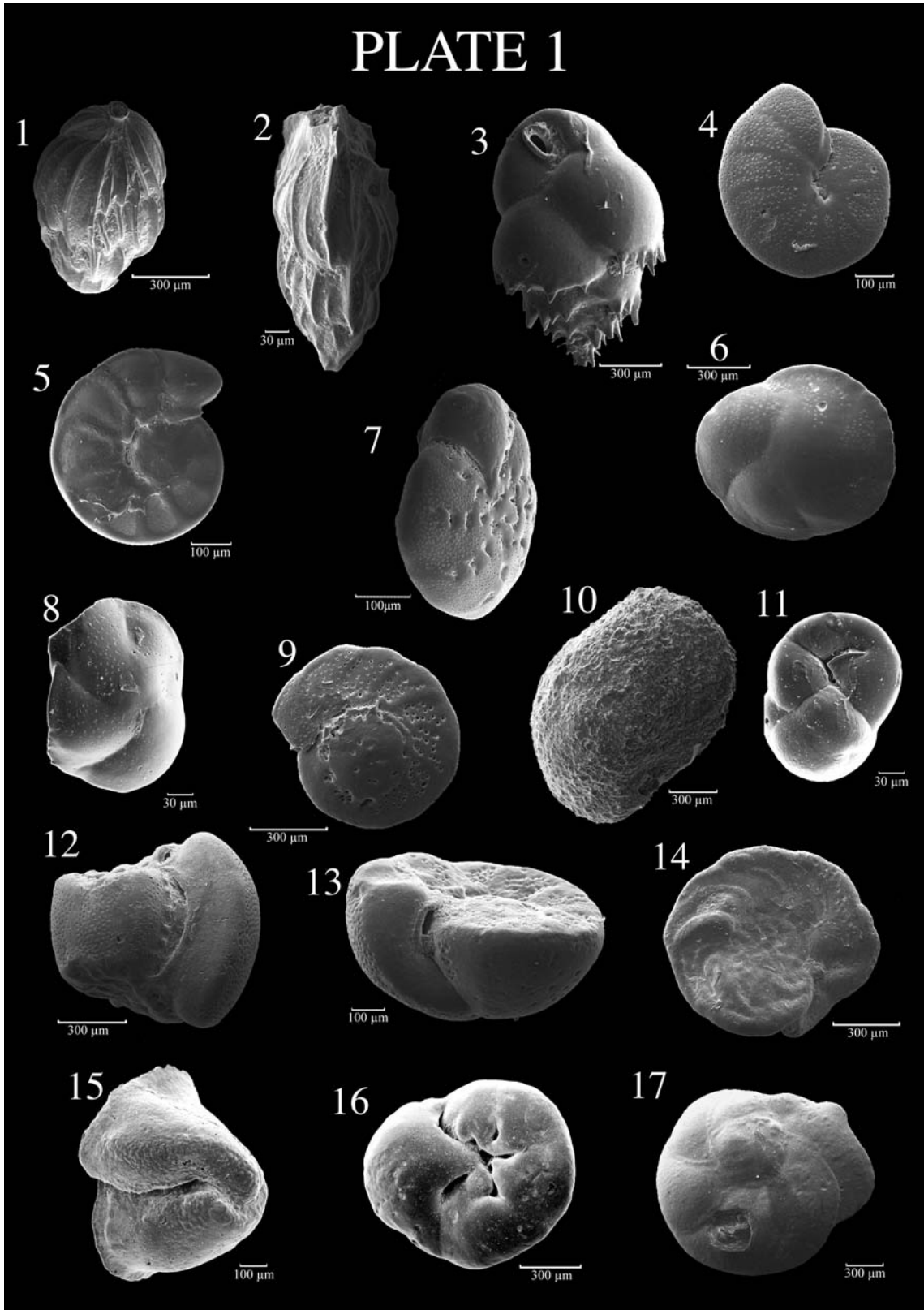
PLATE 1

Fig. 8 Plate 1

Benthic foraminiferal assemblages

The faunal diversity (normalised species numbers) of the on-mound benthic foraminifera is much higher compared to the off-mound site GeoB 6725-1 (Fig. 6), showing values between 32 and 49. The dominance of individual species is generally lower (e.g., *C. teretis*: off-mound maximum >70% compared to on-mound maximum ~23%), which is also described by Coles et al. (1996) for their study in the northern PSB. This indicates that the coral ecosystem offers a habitable life for much more different benthic species with both infaunal and epifaunal lifestyles. As the age model of on-mound core GeoB 6730-1 is insufficient to resolve glacial, interglacial or interstadial periods, the identified groups (glacial group and interglacial group) of the off-mound core are transferred to the counted on-mound species to get an idea of their distribution and variability (Fig. 6).

The glacial group is less abundant in the on-mound record compared to core GeoB 6725-1. During the Holocene, this group behaves similar as in the off-mound core with values between 10 and 20%, but exceeds 20% only within four sections between 120 and 320 cm, with a maximum of 43% at 183 cm (Fig. 6). Though these four sections show higher contributions, they cannot be entirely compared to core GeoB 6725-1 with ~70% typical for fully glacial conditions. Both observations confirm the conclusion that interstadial sediments dominate the entire on-mound record below the Holocene layer already drawn from the $\delta^{18}O$ data. Neither glacial nor interglacial (Holocene) assemblages have a comparably high relative abundance as documented in core GeoB 6725-1.

The interglacial group is less abundant on-mound during the Holocene than in core GeoB 6725-1 with mean values of around 45% (Fig. 6). Maximum abundance (>40%) of this group occurs within the top 118 cm and the section 323–358 cm at the core base, but its abundance generally describes >20% throughout the entire core, except for sections 178–193 and 313 cm. As this group represents high and more continuous flux of organic material within lower oxygen concentrated waters (see above), most of the sediments of the on-mound core can be related to warmer periods, at least interstadials.

In the on-mound samples several species occur, which are not found in the off-mound core or only show accessory contribution (<1%) to the total assemblage. These attached and epibenthic species (*D. coronata*, *G. translucens*, *P. ariminensis*, *C. lobatulus*, *Trifarina bradyi*, *Cicicides refulgens* and *H. sarcophaga*) are also found elsewhere in the NE Atlantic. As they are not common in off-mound samples, they are considered herein as another assemblage, referred to as Mound group. The record of this Mound group varies between 2 and 38% of the total assemblage showing maximum values downcore between 278 and 323 cm. Some of these species also have been recorded in off-mound samples with low abundances. They may be redeposited from the mound.

H. sarcophaga shows only a minor contribution to this assemblage. This species lives attached on *L. pertusa* and shows a parasitic life style (Freiwald and Schönfeld 1996). Some individuals of *H. sarcophaga* have been counted from *L. pertusa* fragments in the fraction >1,000 μm. *D. coronata*, a big (>500 μm) epifaunal species, is reported in waters with high bottom currents and coarse sediment (Schönfeld 1997; Schönfeld and Zahn 2000). Schönfeld (2002b) describes a group of elevated epibenthic species in the Gulf of Cadiz consisting of *Discanomalina semipunctata*, *G. translucens*, *P. ariminensis*, *C. lobatulus*, *C. refulgens* and others. He found coherence between the elevated epibenthos and current intensity of the upper MOW flow. As a similar group of species is recorded here, a higher current intensity and substrates elevated above the sea floor seem to be the controlling factor for the Mound group. The abundance of this group may therefore be related to substrate availability and thus be indicative for a higher coral growth density on Propeller Mound.

Discussion

Environmental setting of Propeller Mound

Late MIS 3

In the off-mound core the transition between MIS 3 and 2 is clearly visible in the abundance of *C. teretis* (Fig. 4). Its record decreases rapidly from >60% relative abundance during late MIS 3 to values around 35% for early MIS 2.

The lower core part is characterised by an enormous sediment supply to the off-mound position. The turbidite at the base of the off-mound core occurred at around 31 kyr BP with sediments eroded and transported from the surrounding Irish Mainland shelf to the east and the Slyne Ridge to the north. Knutz et al. (2001) describe an abrupt increase in basaltic IRD at around 30 kyr BP from a core at the Barra Fan, north of the PSB. They suggest that glaciers reached the shelf-edge transporting terrigenous material from NW Britain into the Rockall Trough area. A similar event most certainly occurred further south possibly resulting in the turbidite sequences at the base of the cores GeoB 6725-1 and GeoB 6719-1 (Dorschel et al. this volume). An advance of the BIIS towards the shelf edge released terrigenous material from Ireland, but also high amounts of shallower shelf sediments are assumed to have been transported downslope.

As high numbers of *E. excavatum* are found within sediments of the off-mound core together with very high sedimentation rates of ~30 cm/kyr, shelf erosional processes continued between 31 and 24 kyr BP, simultaneously with a sea-level lowering of around 50 m (Lambeck et al. 2002) and the extension of the BIIS. Additionally, the occurrence of coral fragments in off-mound core GeoB 6725-1 during late MIS 3 (red stars in

Fig. 4) also suggests that these erosional processes may have affected the elevated mounds (or at least the flanks of the mounds) in the Hovland Mound province, contributing sediments to the off-mound location. Towards MIS 2 shelf erosion decreases, expressed in decreasing numbers of *E. excavatum* (increasing abundance of the glacial group) but probably still persisted to a lesser amount during MIS 2 (Fig. 4).

The last glacial stage

High abundances of *C. teretis* and *C. reniforme*, which are reported in present-day, polar regions (Korsun and Hald 2000), may indicate a very cold bottom water mass. The temperature range where *L. pertusa* is reported to live along the European continental margin is given by Freiwald (2002) with 4–12.5°C. The lower temperature limit corresponds to the occurrence of reefs offshore Norway. Minimum temperatures around *L. pertusa* occurrences within the PSB show little higher values of 7.5°C. GNAIW is reported as the water mass in intermediate depth during the last glacial. According to a coupled climate model simulation, GNAIW shows temperatures 5–6°C cooler compared to recent water masses (Kim et al. 2003). Their model result is coherent with the temperature reconstruction using the difference of benthic δ^{18}O between the Holocene and LGM of the studied cores. The shift corresponds to ∼2.1‰ PDB, resulting in a temperature decrease of around 6°C taking the change in the isotopic composition of bottom waters of 0.8‰ during the LGM for this area into account (Schrag et al. 2002). Additionally, the relation of the glacial group to polar conditions presents a glacial oceanographic setting in the PSB with temperatures <3°C, which is below the habitable limits of *L. pertusa*.

A different composition and source of GNAIW is possibly indicated by increasing contribution of *C. obtusa*, *C. kullenbergi* and *G. subglobosa* to the glacial group during the onset of MIS 2 (decreasing abundance of *C. teretis* in Fig. 4). *C. obtusa* and *G. subglobosa* are reported with increasing abundance during the time of deglaciation and the Holocene at the Faeroe-Shetland Gateway (Rasmussen et al. 2002b). Those species probably show a slightly warmer water mass intrusion into the PSB from a more southerly origin. A shift to higher abundance of almost only *C. teretis* during the deglaciation is related to the intensified formation of the GNAIW in the Norwegian Sea (Manighetti and McCave 1995; Zimmermann 1982) and probably also occurred during late MIS 3 (Fig. 4).

During MIS 2 higher abundances of epifaunal species in the off-mound core are not only an indication of increasing bottom current intensities. For example, Thomas et al. (1995) relate lower abundance of infaunal species (higher abundance of epifaunal taxa) to reduced amounts of organic material reaching the sea floor. Higher abundance of the epifaunal group in core GeoB 6725-1 during the MIS 2 and 3 (Fig. 4) may indicate low glacial surface productivity, but the variations of this group are small, rarely exceeding 10% of the total abundance and a correlation between TOC and the epibenthos group is not visible (Figs. 3 and 4). The influence of benthic foraminifera from Propeller Mound within off-mound sediments is low but detectable. The variations in epibenthic species in the off-mound sample may therefore be the result of erosional features from the elevated mound during glacials. If the oceanographic conditions were not favourable for corals to grow, and coral thickets were not present on the mound to decelerate bottom-near currents, the sediments can be easily washed away and redistribute epibenthic, mound-affected foraminifers in the ambient sedimentary environments.

The Holocene

The benthic foraminiferal assemblage of the Holocene strongly reflects the present-day environmental conditions and oceanographic setting. Species of this group show a great affinity to a high and continuous flux of organic material to the sea-floor (e.g., Loubere 1991; Mackensen et al. 1993; Schönfeld and Zahn 2000), which is considered as a most important environmental factor for the distribution of recent *Uvigerina* species (Thomas et al. 1995; Altenbach et al. 1999). *M. barleeanum* is also highly abundant in organic rich sediments, whereas it shows special demands on quality and concentration of food (Caralp 1989). A generally higher amount of organic material in sediments may be related to higher surface productivity during the Holocene interval, but a correlation between TOC in the sediment with species of the interglacial group is not that evident (Figs. 3 and 4).

The distribution of ENAW and MOW controls the present-day oceanography in 600–800 m water depth, with the MOW being characterised by lower oxygen and higher salinity concentrations. This may cause a deficit in oxygen supply to the near-surface sediments. All endobenthic species of the interglacial group may withstand lower oxygen concentrations in the sediment (Kaiho 1994; Brüchert et al. 2000; Seidenkrantz et al. 2000). Therefore, they could indicate an influence of MOW in the northern PSB during the Holocene. Higher abundance of epibenthic species and *T. angulosa* as well as coarser sediments of the Holocene samples indicate stronger bottom current conditions compared to the glacial.

The Holocene setting with higher surface productivity and a water mass boundary and therefore higher amounts of organic material in the depth of recent coral growth, as well as stronger current intensities seem to be the controlling factor for the recent cold-water coral distribution on Propeller Mound and the Hovland Mound province.

The fate of the Propeller Mound

Higher abundances of epifaunal and attached species have been reported as an indicator for bottom current

intensities (Lutze and Thiel 1989; Linke and Lutze 1993; Hald and Korsun 1997), especially for the MOW in the Gulf of Cadiz (Schönfeld 2002a,b). The abundance of infaunal vs epifaunal taxa is also related to the amount of organic material reaching the ocean bottom (Thomas et al. 1995). On Propeller Mound, where the coral ecosystem produces high amounts of elevated substrates (at least for interglacials or periods of intense coral growth), variations in attached epibenthic foraminifera are rather related to variations in current intensities than productivity. Weston (1985) describes a similar assemblage of benthic foraminifera like the Mound group at the eastern slope of the PSB, where even bigger mounds occur. These mounds of the Belgica Mound province show a much denser coral reef growth on their tops (De Mol et al. 2002). Stronger bottom currents in that area have been documented with mean velocities around 10 cm/s and 10 m above the sea floor, but still > 30% of the measured values exceed 20 cm/s (White 2001). These strong currents are profitable for the corals while feeding on organic material. This also suggests a more favourable habitat for attaching foraminifera on hard substrates, especially for *D. coronata*, *C. lobatulus*, *C. refulgens*, *H. sarcophaga* and *G. translucens*. During the Holocene, these species are relatively rare in samples of the on-mound core and contribute 13% to the interglacial group (Fig. 6). This observation could be due to the restricted coverage of coral reefs on the mound. In a former period of the Late Pleistocene, corresponding to the depth interval of 278–323 cm (Fig. 6), the Propeller Mound seemed to have had a much higher coral density than at present, covering the entire top of the mound, which was favourable for species of the Mound group to settle and to live on the elevated corals. The recent or Late Pleistocene condition of the Propeller Mound describes a declining stage with a general decreasing coral growth. If this situation persists in future, the sediment supply from the surrounding shallower shelf areas especially during transitions from interglacial (interstadial) to glacial stages (e.g., MIS 3/2), which already covered the Magellan Mounds further north, will also bury Propeller Mound.

Conclusions

The results obtained for Propeller Mound and the closer vicinity clearly reflect the important environmental control responsible for the growth and retreat of corals steered by oceanographic and climatic factors (Freiwald 1998, 2002; White this volume). Under fully glacial conditions the environmental setting was beyond the habitable range of *Lophelia* corals with temperatures below 4°C, low-current intensities supporting high-sediment accumulation and a homogenous intermediate water mass, which does not support nutrient enrichment in the depth of the carbonate mounds. Upto now for no coral from the Celtic Margin an age representing the LGM has been obtained, indicating that no coral lived

in this region. Thus, there was also no skeletal framework to stabilise the fine-grained sediments deposited under such conditions.

During terminations, when the sea-level rose and the glaciers retreated from Ireland, ENAW and MOW regain their present characteristics. Enhanced currents removed the unstabilised sediments from the mound, which is expressed in several hiatuses covering glacial periods of core GeoB 6730-1. De Mol et al. (2002) and Freiwald (2002) discussed the possibility of coral larvae entering the PSB with the inflow of the MOW during the terminations, as *Lophelia* is highly abundant within the Mediterranean during the glacials but at present is nearly absent (Delibrias and Taviani 1985). With an oceanographic regime comparable to the present-day setting, the corals were able to (re-) colonise the elevated structure and the mound proceeded to grow.

The glacial–interglacial cycle with changing environmental conditions seems to be one mechanism driving the development of the carbonate mounds along the Celtic Margin. Interglacial/interstadial growth, glacial retreat and resettlement of corals during terminations with removal of glacial sediments are combined in a model describing the Mound Factory (Fig. 7). This model accounts for the time, when the North Atlantic experienced the Northern Hemisphere Glaciation, which started between 3.1 and 2.5 million years BP (Shackleton et al. 1995; Haug et al. 2001). However, it is still under debate, which trigger was responsible for the initial mound development. Only a deep drilling campaign through the base of such carbonate mounds will shed some light into the debate about the onset and the trigger of mound development.

Appendix 1

Faunal reference list of benthic foraminiferal species considered in this paper (in alphabetical order):

Bulimina marginata d'ORBIGNY = *B. marginata* d'ORBIGNY, 1826—Plate 1, Fig. 3. Feyling-Hanssen et al. (1971, Plate 6, Figs.17–20), Oki (1989, Plate 11, Fig. 3), Collins (1989, Plate 1, Fig. 4).

Cassidulina laevigata d'ORBIGNY = *C. laevigata* d'ORBIGNY, 1826—Plate 1, Fig. 6. Feyling-Hanssen et al. (1971, Plate 7, Figs. 20–21; Plate 18, Fig. 12),

Mackensen and Hald ([1988](#), Plate 1, Figs. [1–7](#)), Schiebel ([1992](#), Plate 2, Fig. 11), Heß ([1996](#), Plate 13, Fig. 8).

Cassidulina obtusa WILLIAMSON = *C. obtusa* WILLIAMSON, 1858. Hald and Steinsund ([1992](#), Plate 2, Fig. [3](#)), Gooday and Hughes ([2002](#), Plate 2, Fig. d).

Cassidulina reniforme NØRVANG = *C. reniforme* NØRVANG, 1945. Thomas et al. ([1990](#), Plate 4, Figs. 13 and 14; Plate 10, Fig. 10).

Cassidulina teretis TAPPAN = *C. teretis* TAPPAN, 1951—Plate 1, Fig. 8. Mackensen and Hald ([1988](#), Plate 1, Figs. 8–15), Gooday and Hughes ([2002](#), Plate 2, Fig. e).

Cibicides lobatulus (WALKER& JACOB) = *Nautilus lobatulus* WALKER& JACOB, 1889—Plate 1, Fig. 13. Feyling-Hanssen et al. ([1971](#), Plate 9, Figs. 9–14), Thies ([1991](#), Plate 17, Fig. [4](#); Plate 18, Figs. 1–20), Struck ([1992](#), Plate 5, Fig. [1](#)), Schönfeld ([2002a](#), [b](#), Plate1, Figs. [2](#) and [3](#)).

Cibicides refulgens MONTFORT = *C. refulgens* MONTFORT, 1808—Plate 1, Fig. 15. Schönfeld ([2002a](#), [b](#), Plate 1, Figs. 11 and 12), Weston ([1985](#), Plate 2, Fig. 8).

Cibicidoides kullenbergi (PARKER) = *Cibicides kullenbergi* PARKER, 1953—Plate 1, Fig. 9. Caralp ([1985](#), Plate 6, Figs. 8–11).

Discanomalina coronata (PARKER and JONES) = *Anomalina coronata* PARKER and JONES, 1857—Plate 1, Fig. 12. Schönfeld ([2002a](#), [b](#), Plate 1, Fig. 14).

Elphidium excavatum (TERQUEM) = *Polystomella excavata* TERQUEM, 1875—Plate 1, Fig. [7](#). Thomas et al. ([1990](#), Plate 4, Figs. [5–7](#); Plate 7, Figs. [1–3](#); Plate 9, Figs. 19–22), Thies ([1991](#), Plate 19, Fig. [5](#)).

Gavelinopsis translucens (PHLEGER& PARKER) = *G. translucens* PHLEGER& PARKER, 1951. Gooday and Hughes ([2002](#), Plate 1, Fig. A), Heß ([1996](#), Plate 15, Figs. [1](#) and [2](#)), Timm ([1992](#), Plate 7, Fig. 12), Schiebel ([1992](#), Plate 4, Fig. [5](#)).

Globocassidulina subglobosa (BRADY) = *Cassidulina subglobosa* BRADY, 1881—Plate 1, Fig. 11. Struck ([1992](#), Plate 3, Fig. [2](#)), Timm ([1992](#), Plate 6, Fig. 20), Heß ([1996](#), Plate 13, Fig. 14), Ohkushi et al. ([2000](#), Plate 2, Fig. 8).

Hyalinea balthica (SCHRÖTER) = *Nautilus balthicus* SCHRÖTER, 1783—Plate 1, Fig. [5](#). Oki ([1989](#), Plate 17, Fig. [6](#)).

Hyrrokkin sarcophaga CEDHAGEN = *H. sarcophaga* CEDHAGEN, 1994, Plate 1, Figs. 16 and 17. Freiwald and Schönfeld ([1996](#), Plate 202, Fig. [2](#)a; Plate 205, Fig. [5](#)a).

Melonis barleeanum (WILLIAMSON) = *Nonionina barleeana* WILLIAMSON, 1858—Plate 1, Fig. [4](#). Struck ([1992](#), Plate 4, Fig. [6](#)), Timm ([1992](#), Plate 6, Fig. [6](#)), Heß ([1996](#), Plate 13, Fig. [5](#)).

Planulina ariminensis d'ORBIGNY = *P. ariminensis* d'ORBIGNY, 1826—Plate 1, Fig. 14. Feyling-Hanssen et al. ([1971](#), Plate 9, Figs. [4–6](#)), Heß ([1996](#), Plate 16, Fig. 8).

Sigmoilopsis woodi ATKINSON = *S. woodi* ATKINSON, 1968—Plate 1, Fig. 10. Ellis and Messina ([1940](#)–1978; http://www.micropress.org).

Trifarina angulosa (WILLIAMSON) = *Uvigerinaangulosa* WILLIAMSON, 1858—Plate 1, Fig. [2](#). Oki ([1989](#), Plate 12, Fig. 10), Schiebel ([1992](#), Plate 3, Fig. [1](#)), Timm ([1992](#), Plate 6, Fig. [5](#)).

Trifarina bradyi CUSHMAN = *T. bradyi* CUSHMAN, 1923. Weston ([1985](#), Plate 1, Fig. [5](#)), Heß ([1996](#), Plate 10, Fig. 14).

Uvigerina mediterranea HOFKER = *U. mediterranea* HOFKER, 1932—Plate 1, Fig. [1](#). Thies ([1991](#), Plate 17, Fig. [3](#)), Schiebel ([1992](#), Plate 3, Fig. [7](#)).

Uvigerina peregrina CUSHMAN = *U. peregrina* CUSHMAN, 1923. Feyling-Hanssen et al. ([1971](#), Plate 7, Figs. 9–11), Timm ([1992](#), Plate 6, Fig. [2](#)), Heß ([1996](#), Plate 11, Figs. [2](#) and [3](#)), Ohkushi et al. (2000, Plate 2, Fig. [4](#)).

Appendix 2

Interglacial group

1. *Uvigerina mediterranea* HOFKER, 1932. Sample: GeoB 6725-1, 23 cm, fraction 250–500 μm.
2. *Trifarina angulosa* (WILLIAMSON, 1858). Sample: GeoB 6725-1, 23 cm, fraction 250–500 μm.
3. *Bulimina marginata* d'ORBIGNY, 1826. Sample: GeoB 6725-1, 368 cm, fraction 250–500 μm.
4. *Melonis barleeanum* (WILLIAMSON, 1858). Sample: GeoB 6725-1, 338 cm, fraction 250–500 μm.
5. *Hyalinea balthica* (SCHRÖTER, 1783). Sample: GeoB 6725-1, 13 cm, fraction 250–500 μm.
6. *Cassidulina laevigata* d'ORBIGNY, 1826. Sample: GeoB 6725-1, 253 cm, fraction 125–250 μm.

Glacial group

7. *Elphidium excavatum* (TERQUEM, 1875). Sample: GeoB 6725-1, 338 cm, fraction 250–500 μm.
8. *Cassidulina teretis* TAPPAN, 1951. Sample: GeoB 8059-1, 0–1 cm, fraction 125–250 μm.
9. *Cibicidoides kullenbergi* (PARKER, 1953). Sample: GeoB 6725-1, 338 cm, fraction 250–500 μm.
10. *Sigmoilopsis woodi* ATKINSON, 1968. Sample: GeoB 6730-1, 3 cm, fraction 500–1,000 μm.
11. *Globocassidulina subglobosa* (BRADY, 1881). Sample: GeoB 8045-1, 0–1 cm, fraction 125–250 μm.

Mound group

12. *Discanomalina coronata* (PARKER& JONES, 1857). Sample: GeoB 6730-1, 3 cm, fraction 500–1,000 μm.
13. *Cibicides lobatulus* (WALKER& JACOB, 1889). Sample: GeoB 6725-1, 58 cm, fraction 500–1,000 μm.
14. *Planulina ariminensis* d'ORBIGNY, 1826. Sample: GeoB 6730-1, 3 cm, fraction 500–1,000 μm.
15. *Cibicides refulgens* MONTFORT, 1808. Sample: GeoB 8045-1, 0–1 cm, fraction 500–1,000 μm.

16. *Hyrrokkin sarcophaga* CEDHAGEN, 1994. Sample: GeoB 8045-1, 0–1 cm, fraction 500–1,000 μm.
17. *Hyrrokkin sarcophaga* CEDHAGEN, 1994. Sample: GeoB 6730-1, 3 cm, fraction > 1,000 μm.

References

Altenbach AV (1992) Verbreitungsmuster benthischer Foraminiferen im Arktischen Ozean und in glazialen und interglazialen Sedimenten des Europäischen Nordmeeres. Habilitationsschrift, Christian-Albrechts-Universität, p 95

Altenbach AV, Pflaumann U, Schiebel R, Thies A, Timm S, Trauth M (1999) Scaling percentages and distributional patterns of benthic foraminifera with flux rates of organic carbon. J Foraminifer Res 29(3):173–185

Auffret G, Zaragosi S, Dennielou B, Cortijo E, Van Rooij D, Grousset F, Pujol C, Eynaud F, Siegert M (2002) Terrigenous fluxes at the Celtic margin during the last glacial cycle. Mar Geol 188:79–108

Bond G, Lotti R (1995) Iceberg discharges into the north Atlantic on millennial time scales during the last glaciation. Science 267:1005–1009

Bowen DQ, Phillips FM, McCabe AM, Knutz PC, Sykes GA (2002) New data for the last glacial maximum in Great Britain and Ireland. Quat Sci Rev 21:89–101

Brüchert V, Perez ME, Lange CB (2000) Coupled primary production, benthic foraminiferal assemblage, and sulphur diagenesis in organic-rich sediments of the Benguela upwelling system. Mar Geol 163:27–40

Caralp MH (1985) Quaternary calcareous benthic foraminifers, Leg 80. In: de Graciansky PC, Poag CW et al (eds) Initial reports of the deep sea drilling project. US Government Printing Office, Washington, pp725–755

Caralp MH (1989) Size and morphology of the benthic foraminifer Melonis barleeanum: relationships with marine organic matter. J Foraminifer Res 19(3):235–245

Cheng H, Adkins J, Edwards RL, Boyle EA (2000) U–Th dating of deep-sea corals. Geo Cosmo Acta 64(14):2401–2416

Coles GP, Ainsworth NR, Whatley RC, Jones RW (1996) Foraminifera and ostracoda from quaternary carbonate mounds associated with gas seepage in the Porcupine Basin, offshore western Ireland. Rev Esp Micropaleontol 28(2):113–151

Collins LS (1989) Relationship of environmental gradients to morphologic variation within *Bulimina aculeata* and *Bulimina marginata*, Gulf of Maine area. J Foraminifer Res 19(3):222–234

Conradsen K (1993) Recent benthic foraminifera in the Kattegat, Scandinavia: distributional pattern and controlling parameters. Boreas 22:367–382

Delibrias G, Taviani M (1985) Dating the death of Mediterranean deep-sea scleractinian corals. Mar Geol 62:175–180

De Mol B (2002) Development of coral banks in Porcupine Seabight (SW Ireland): a multidisciplinary approach. Ph.D. thesis, University Gent, p 363

De Mol B, Van Rensbergen P, Pillen S, Van Herreweghe K, Van Rooij D, McDonnell A, Huvenne V, Ivanov M, Swennen R, Henriet JP (2002) Large deep-water coral banks in the Porcupine Basin, southwest of Ireland. Mar Geol 188:193–231

Dorschel B, Hebbeln D, Rüggeberg A, Dullo C (this volume) Carbonate budget of a cold-water carbonate mound: Propeller Mound, Porcupine Seabight. Int J Earth Sci

Duplessy JC, Shackleton NJ, Fairbanks RG, Labeyrie LD, Oppo D, Kallel N (1988) Deep water source variations during the last climatic cycle and their impact on global deep water circulation. Paleoceanography 3:343–360

Ellet DJ, Edwards A, Bowers R (1986) The hydrography of the Rockall Channel—an overview. Proc Royal Soc Edinb 88(B):61–81

Ellis BE, Messina AR (1940–1978) Catalogue of Foraminifera. American Museum of Natural History, New York (ISBN 0-913424-34-X)

Eyles N, McCabe AM (1989) The Late Devensian (< 22,000 BP) Irish Sea Basin: the sedimentary record of a collapsed ice sheet margin. Quat Sci Rev 8:307–351

Feyling-Hanssen RW, Joergensen JA, Knudsen KL, Andersen A-LL (1971) Late Quaternary foraminifera from Vendsyssel, Denmark and Sandnes, Norway. Bull Geol Soc Denmark 21(2–3):67–317

Freiwald A (1998) Geobiology of *Lophelia pertusa* (scleractinian) reef in the North Atlantic. Habilitationsschrift, Department of Geosciences, University of Bremen, p 116

Freiwald A (2002) Reef-forming cold-water corals. In: Wefer G, Hebbeln D, Jørgensen BB, Schlüter M, van Weering T (eds) Ocean margin systems. Springer, Berlin Heidelberg New York, p 495

Freiwald A, Schönfeld J (1996) Substrate pitting and boring pattern of *Hyrrokkin sarcophaga* Cedhagen, 1994 (foraminifera) in a modern deep-water coral reef mound. Mar Micropaleontol 28:199–207

Freiwald A, Shipboard Party (2002) Cruise Report RV POSEIDON Cruise 292, Reykjavik–Galway, 15 July–4 August 2002

Freiwald A, Dullo C, Shipboard Party (2000) Cruise Report RV POSEIDON Cruise 265, Thorshavn–Galway–Kiel, 13 September–1 October 2000

Games KP (2001) Evidence of shallow gas above the Connemara oil accumulation, Block 26/28, Porcupine Basin. In: Shannon PM, Haughton PDW, Corcoran DV (eds) The petroleum exploration of Ireland's offshore basins. Geol Soc Spec Publ 188:361–373

Gooday AJ, Hughes JA (2002) Foraminifera associated with phytodetritus deposits at a bathyal site in the northern Rockall Trough (NE Atlantic): seasonal contrasts and a comparison of stained and dead assemblages. Mar Micropaleontol 46:83–110

Grousset F, Pujol C, Labeyrie L, Auffret G, Boelaert A (2000) Were the North Atlantic Heinrich events triggered by the behaviour of the European ice sheet? Geology 28(2):123–126

Hald M, Korsun S (1997) Distribution of modern benthic foraminifera from fjords of Svalbard, European Arctic. J Foraminifer Res 27:101–122

Hald M, Steinsund PT (1992) Distribution of surface sediment benthic foraminifera in the southwestern Barents Sea. J Foraminifer Res 22(4):347–362

Hald M, Steinsund PI, Dokken T, Korsun S, Polyak L, Aspeli R (1994) Recent and late Quaternary distribution of *Elphidium excavatum* f. *clavatum* in the Arctic Seas. Cushman Found Spec Publ 32:141–153

Haug GH, Tiedemann R, Zahn R, Ravelo AC (2001) Role of Panama uplift on oceanic freshwater balance. Geology 29(3):207–210

Henriet J-P, De Mol B, Pillen S, Vanneste M, Van Rooij D, Versteeg W, Croker PF, Shannon PM, Unnithan V, Bouriak S, Chachkine P (1998) Gas hydrate crystals may help build reefs. Nature 391:648–649

Heß S (1996) Rezente benthische Foraminiferen in Sedimenten des Schelfes und oberen Kontinentalhanges im Golf von Guinea (Westafrika). Berichte Geologisch-Paläontologisches Institut, Christian-Albrechts-Universität zu Kiel 91:173

Huvenne VAI, Blondel Ph, Henriet J-P (2002) Textural analyses of sidescan sonar imagery from two mound provinces in the Porcupine Seabight. Mar Geol 189(3–4):323–341

Jones RL, Keen DH (1993) Pleistocene environments in the British Isles. Chapman& Hall, London, p 368

Kaiho K (1994) Benthic foraminiferal dissolved-oxygen index and dissolved-oxygen levels in the modern ocean. Geology 22:719–722

Kim S-J, Flato GM, Boer GJ (2003) A coupled climate model simulation of the last glacial maximum, Part 2: approach to equilibrium. Clim Dynam 20:635–661

Knutz PC, Austin WEN, Jones EJW (2001) Millennial-scale depositional cycles related to British Ice Sheet variability and North Atlantic paleocirculation since 45 kyr B.P., Barra Fan, UK margin. Paleoceanography 16(1):53–64

Korsun SA, Polyak LV (1989) Distribution of benthic foraminiferal morphogroups in the Barents Sea. Oceanology 29(5):838–844

Korsun S, Hald M (2000) Seasonal dynamics of benthic foraminifera in a glacially fed fjord of Svalbard, European Arctic. J Foraminifer Res 30:251–271

Lambeck K, Esat TM, Potter E-K (2002) Links between climate and sea levels for the past three million years. Nature 419:199–206

Linke P, Lutze GF (1993) Microhabitat preferences of benthic foraminifera—a static concept or a dynamic adaption to optimise food acquisition?. Mar Micropaleontol 20:215–234

Loubere P (1991) Deep-sea benthic foraminiferal assemblage response to a surface ocean productivity gradient: a test. Paleoceanography 6(2):193–204

Lutze GF (1980) Depth distribution of benthic foraminifera on the continental margin off NW Africa. "METEOR" Res Results 32(C):31–80

Lutze GF, Thiel H (1989) Epibenthic foraminifera from elevated microhabitats: *Cibicidoides wuellerstorfi* and *Planulina ariminensis*. J Foraminifer Res 19(2):153–158

Mackensen A, Hald M (1988) *Cassidulina teretis* TAPPAN and *C. laevigata* d'ORBIGNY: their modern and late quaternary distribution in Northern seas. J Foraminifer Res 18(1):16–24

Mackensen A, Fütterer DK, Grobe H, Schmiedl G (1993) Benthic foraminiferal assemblages from the eastern South Atlantic Polar Front region between 35° and 57°S: distribution, ecology and fossilization potential. Mar Micropaleontol 22:33–69

Mackensen A, Schmidl G, Harloff J, Giese M (1995) Deep-sea foraminifera in the South Atlantic Ocean: ecology and assemblage generation. Micropaleontology 41(4):342–358

Manighetti B, McCave IN (1995) Late glacial and Holocene palaeocurrents around Rockall Bank, NE Atlantic Ocean. Paleoceanography 10(3):611–626

McCartney MS, Mauritzen C (2001) On the origin of the warm inflow to the Nordic Seas. Prog Oceanogr 51:152–214

Mohn C (2000) Über Wassermassen und Strömungen im Bereich des europäischen Kontinentalrandes westlich von Irland. Ph.D. thesis, University Hamburg, Germany, p 134

Murray JW (1991) Ecology and palaeoecology of benthic foraminifera. Longman Scientific & Technical, Essex

Nadeau MJ, Schleicher M, Grootes P, Erlenkeuser H, Gottolong A, Mous DJW, Sarnthein M, Willkomm N (1997) The Leibnitz–Labor AMS facility at the Christian–Albrechts University, Kiel, Germany. Nucl Instrum Methods Phys Res 123:22–30

Nagy Y (1965) Foraminifera in some bottom samples from shallow waters in Vestspitsbergen. Nor Polarinst Å rb 1963:109–125

New AL, Jia Y, Coulibaly M, Dengg J (2001) On the role of the Azores current in the ventilation of the North Atlantic Ocean. Prog Oceanogr 48:163–194

Ohkushi K, Thomas E, Kawahata H (2000) Abyssal benthic foraminifera from the northwestern Pacific (Shatsky Rise) during the last 298 kyr. Mar Micropaleontol 38:119–147

Oki K (1989) Ecological analysis of benthonic foraminifera in Kagoshima Bay, South Kyushu, Japan. South Pacific Stud 10(1):191

Oppo D, Lehman S (1993) Mid-depth circulation of the sub-polar North Atlantic during the last glacial maximum. Science 259:1148–1152

Pollard RT, Griffiths MJ, Cunningham SA, Read JF, Perez FF, Rios AF (1996) Vivaldi 1991—a study of the formation, circulation and ventilation of Eastern North Atlantic Water. Prog Oceanog 37:167–192

Rasmussen TL, Thomsen E, van Weering TCE, Labeyrie L (1996) Rapid changes in surface and deep water conditions at the Faeroe Margin during the last 58,000 years. Paleoceanography 11(6):757–771

Rasmussen TL, Thomsen E, Troelstra SR, Kuijpers A, Prins MA (2002a) Millennial-scale glacial variability versus Holocene stability: changes in planktic and benthic foraminifera faunas and ocean circulation in the North Atlantic during the last 60 000 years. Mar Micropaleontol 47:143–176

Rasmussen TL, Bäckström D, Heinemeier J, Klitgaard-Kristensen D, Knutz PC, Kuijpers A, Lassen S, Thomsen E, Troelstra SR, van Weering TCE (2002b) The Faroe–Shetland Gateway: late quaternary water mass exchange between the Nordic seas and the northeastern Atlantic. Mar Geol 188:165–192

Sarnthein M, Jansen W, Weinelt M, Arnold M, Duplessy J-C, Erlenkeuser H, Flatøy A, Johannessen G, Johannessen T, Jung S, Koc N, Labeyrie L, Maslin M, Pflaumann U, Schulz H (1995) Variations in Atlantic surface ocean paleoceanography, 50°–80°N: a time-slice record of the last 30,000 years. Paleoceanography 10(6):1063–1094

Schiebel R (1992) Rezente benthische Foraminiferen in Sedimenten des Schelfes und oberen Kontinentalhanges im Golf von Guinea (Westafrika). Berichte Geologisch-Paläontologisches Institut, Christian-Albrechts Universität zu Kiel 51179

Schönfeld J (1997) The impact of the Mediterranean outflow water (MOW) on benthic foraminiferal assemblages and surface sediments at the southern Portuguese continental margin. Mar Micropaleontol 29:211–236

Schönfeld J (2002a) Recent benthic foraminiferal assemblages in deep high-energy environments from the Gulf of Cadiz (Spain). Mar Micropaleontol 44:141–162

Schönfeld J (2002b) A new benthic foraminiferal proxy for near-bottom current velocities in the Gulf of Cadiz, northeastern Atlantic Ocean. Deep-Sea Res I 49:1853–1875

Schönfeld J, Zahn R (2000) Late Glacial to Holocene history of the Mediterranean outflow. Evidence from benthic foraminiferal assemblages and stable isotopes at the Portuguese margin. Palaeogeogr Palaeocl Palaeoecol 159:85–111

Schrag DP, Adkins JF, McIntyre K, Alexander JL, Hodell DA, Charles CD, McManus JF (2002) The oxygen isotopic composition of seawater during the last glacial maximum. Quat Sci Rev 21:331–342

Seidenkrantz M-S, Kouwenhoven TJ, Jorissen FJ, Shackleton NJ, van der Zwaan GJ (2000) Benthic foraminifera as indicators of changing Mediterranean-Atlantic water exchange in the late Miocene. Mar Geol 163:387–407

Shackleton NJ, Hall M, Pate D (1995) Pliocene stable isotope stratigraphy of Site 846. Proc Ocean Drilling Program Sci Results 138:337–357

Steinsund PI, Hald M (1994) Recent calcium carbonate dissolution in the Barents Sea; paleogeographic applications. Mar Geol 117:303–316

Struck U (1992) Zur Paläo-Ökologie benthischer Foraminiferen im Europäischen Nordmeer während der letzten 600.000 Jahre. Berichte aus dem Sonderforschungsbereich 313, Christian-Albrechts-Universität zu Kiel 38129

Stuiver M, Reimer PJ (1993) Extended ^{14}C data base and revised CALIB 3.0 14C age calibration program. Radiocarbon 35:215–230

Stuiver M, Reimer PJ, Braziunas TF (1998) Revised dataset. Radiocarbon 40:1127–1151

Thies A (1991) Die Benthosforaminiferen im Europäischen Nordmeer. Berichte aus dem Sonderforschungsbereich 313, Christian-Albrechts-Universität zu Kiel 3197

Thomas FC, Medioli FS, Scott DB (1990) Holocene and latest Wisconsinan benthic foraminiferal assemblages and paleocirculation history, Lower Scotian slope and rise. J Foraminifer Res 20(3):212–245

Thomas E, Booth L, Maslin M, Shackleton NJ (1995) Northeastern Atlantic benthic foraminifera during the last 45,000 years: changes in productivity seen from the bottom up. Paleoceanography 10(3):545–562

Timm S (1992) Rezente Tiefsee-Benthosforaminiferen aus Oberflächensedimenten des Golfes von Guinea (Westafrika)—Taxono-

mie, Verbreitung, Ökologie und Korngrößenfraktionen. Berichte Geologische-Paläontologisches Institut Christian-Albrechts-Universität zu Kiel 59192

Veum T, Jansen E, Arnold M, Beyer I, Duplessy J-C (1992) Water mass exchange between the North Atlantic and the Norwegian Sea during the past 28,000 years. Nature 356:783–785

Voelker AHL, Sarnthein M, Grootes PM, Erlenkeuser H, Laj C, Mazaud A, Nadeau M-J, Schleicher M (1998) Correlation of marine ^{14}C ages from the Nordic Seas with the GISP2 isotope record: implications for radiocarbon calibration beyond 25 ka BP. Radiocarbon 40(1,2):517–534

Weston JF (1985) Comparison between recent benthic foraminiferal faunas of the Porcupine Seabight and Western Approaches Continental Slope. J Micropaleontol 4(2):165–183

White M (2001) Hydrography and physical dynamics at the NE Atlantic Margin that influence the Deep Water Cold Coral Reef Ecosystem, Department of Oceanography, NUI, Galway

White M (this volume) The hydrography of the Porcupine Bank and Sea Bight and associated carbonate mounds. Int J Earth Sci

Zimmermann HB (1982) Fine-grained sediment distribution in the Late Pleistocene/Holocene North Atlantic. Bull Inst Geol Bassin Aquitaine 31: 337–357